Vol. 7(24), Apr. 2017, PP. 3411-3422

Contents list available at IJMEC

International Journal of Mechatronics, Electrical and Computer Technology (IJMEC)

Journal Homepage: www.aeuso.org

PISSN: 2411-6173 - EISSN: 2305-0543

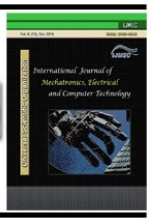

Design and Analysis Of Control Using Indirect Field-Oriented Controller for Induction Motors

Peyman Jabraelzade[1*] and Neda Pourghanbarkalaibar[2]

[1]*Department of Mechatronics Ahar branch, Islamic Azad university, Ahar, Iran*

[2]*Department of Electrical Engineering Ahar branch, Islamic Azad university, Ahar, Iran*

Phone Number: *+98-9147734542*

****Corresponding Author's E-mail:*** *p-jabraelzade@iau-ahar-ac.ir*

Abstract

TAn asynchronous motor type of an induction motor is an AC electric motor in which the electric current in the rotor needed to produce torque is obtained by electromagnetic induction from the magnetic field of the stator winding. An induction motor can therefore be made without electrical connections to the rotor as are found in universal, DC and synchronous motors. Although the design and construction inductive engines easier than DC Motors, but for velocity control and in various forms of inductive engines need more comprehensive knowledge in the design and construction of this kind. In the functions of the low - speed and also under the control of the situation, the use of sensors Hall due to various errors, with the desired results. Option in this case, Using Indirect Method Vector Control of Induction Motor that do not use the direct measurement of the air gap flux. This paper presents the vector control of induction motor using indirect method. Fundamental principles of vector control and dynamic mathematical model of induction motor are discussed. An algorithm for the implementation of vector control is lucidly presented. Analysis of the sensitivity of the parameters in the best way possible, the answer was dynamic and steady state errors. The results are validated using MATLAB/SIMULINK.

Keywords: *Dynamic behavior, stability, dynamic response, indirect field-oriented control, induction motor*.

1. Introduction

A flurry of various controllers was introduced in the late 1980s through today. This was due to the fact that variable frequency drives have become extremely popular since the advent of power electronics in the 1960s. The use of the bipolar junction transistor (BJT) and then the field effect transistor (FET) have enabled the conversion between different types of power sources. A detailed comparison of different induction motor drives is given in [1], including volts-per-hertz (V/Hz), FOC, DTC, direct self control (DSC), and DTC with space vector modulation (DTC-SVM). This comparison mentions advantages and disadvantages relative to steady-state measures, such as phase current peaks, current and torque harmonics, and switching frequency variation. Structural measures, such as the need for flux observers, and decoupling the torque and flux commands, are also presented. Cruz

Article History:

Received Date: Sep. 03, 2016

Accepted Date: Jan. 11, 2017

Available Online: Mar. 06, 2017

et al [2] compare FOC, DTC and input/output linearization based on steady-state torque ripple, current peak, and switching frequency to name a few. They conclude that FOC and DTC are "good" in dynamic response, and that the parameter sensitivities are "low" and "medium" in DTC and FOC, respectively. Wolbank et al [3] compare low and zero-speed applications of DTC and sensorless FOC. They study steady-state stability and speed overshoot, where FOC shows slower dynamics but better steady-state tracking compared to DTC. As both FOC and DTC have drawbacks, an interesting combination of DTC and FOC is presented in [4]. The resulting direct torque and stator flux control method (DTFC) does not use voltage modulation, current regulation loops, coordinate transformations, or voltage decoupling. Vasudevan and Arumugam [5] compare IFOC to DFOC along with classical DTC-SVM and direct torque neuro-fuzzy control using MATLAB/Simulink. Stator voltages and currents, angular velocity, torque, and flux responses to a change in torque or angular velocity, are compared. The effect of parameter variation, such as stator resistance variation due to temperature increases, is also discussed in relation to the DTC control method.

2. Induction Motor Dynamic Model

The following set of seven time-varying equations in (1) from [6] are known collectively as the induction motor dynamic model in the arbitrary reference frame. The variables with the subscript s indicate that it is a stator variable, while the subscript r shows it is a rotor quantity. It should be noted that this model is exclusively for variables in the dq0 plane rather than the time-variant plane. The motor terminal voltages are indicated by v, the currents by i, the flux linkages by λ, and the rotor speed by r_ω. The number of pole pairs is given by p_n , the load torque by T_{load}, and the shaft moment of inertia by J.

$$\frac{d\lambda_{qs}}{dt} = -r_s i_{qs} - \omega\lambda_{ds} + v_{qs}$$
$$\frac{d\lambda_{qs}}{dt} = -r_s i_{ds} + \omega\lambda_{ds} + v_{ds}$$
$$\frac{d\lambda_{os}}{dt} = -r_s i_{os} + v_{os}$$
$$\frac{d\lambda_{qr}}{dt} = -r_r i_{qr} - \left(\omega - n_p\omega_r\right)\lambda_{dr} + v_{qr}$$
$$\frac{d\lambda_{dr}}{dt} = -r_r i_{dr} + \left(\omega - n_p\omega_r\right)\lambda_{qr} + v_{ds}$$
$$\frac{d\lambda_{or}}{dt} = -r_r i_{or} + v_{or}$$
$$\frac{d\omega_r}{dt} = \frac{3}{2}\frac{n_p}{J}\left(\lambda_{ds} i_{qs} - \lambda_{qs} i_{ds}\right) - \frac{T_{load}}{J} \quad (1)$$

3. Indirect Field-Oriented Control

Indirect field-oriented control, or IFOC, is the most common IM drive because of its use of moderate amounts of parameter information to give it respectable performance while also not requiring a high level of sophistication. Field-oriented control (FOC) was introduced by Blaschke in 1971 [7, 8]. FOC was created to imitate the control of a separately excited dc motor. In a similar fashion to the dc motor, the FOC drive keeps the rotor flux perpendicular to the stator flux to get the maximum output torque possible. The big advantage of FOC is that the flux and the torque can be decoupled by insuring that the other is in steady state. In this fashion, the dynamics can be independently controlled by the user. Because of this, the classical feedback control can be used to obtain desired motor performance. The basic attribute of IFOC is that it uses an estimate of the rotor flux in determining the next state of the

inverter. In particular, it uses the angle of the rotor flux to determine where the flux is in vector-space. The angle is calculated by (2).

$$\rho = tan^{-1}\left(\frac{\lambda_{qr}}{\lambda_{dr}}\right) \quad (2)$$

This flux vector angle is then used in a matrix transformation that converts the stator current and rotor flux values into a new state space $\{\omega_r, {}^{\psi}, i_q, i_d, \rho\}$ where:

$$\omega_r = \omega_r$$
$$\square = \sqrt{\lambda_{qr+\lambda_{dr}}^2}$$
$$i_q = \frac{\lambda_{dr} i_{qs} - \lambda_{qr} i_{ds}}{\psi}$$
$$i_d = \frac{\lambda_{dr} i_{ds} + \lambda_{qr} i_{qs}}{\psi}$$
$$\rho = tan^{-1}\left(\frac{\lambda_{qr}}{\lambda_{dr}}\right) \quad (3)$$

This is equivalent to using the following matrix conversion for the same currents and flux values:

$$\begin{pmatrix} i_d \\ i_q \end{pmatrix} = \Gamma \begin{pmatrix} i_{ds} \\ i_{qs} \end{pmatrix}$$
$$\begin{pmatrix} \psi \\ o \end{pmatrix} = \Gamma \begin{pmatrix} \lambda_{dr} \\ \lambda_{qr} \end{pmatrix}$$
$$\Gamma = \begin{pmatrix} cos(p) & sin(p) \\ -sin(p) & cos(p) \end{pmatrix} \quad (4)$$

If we let the vector be equal to that in (5),

$$\begin{pmatrix} v_d \\ v_q \end{pmatrix} = \sigma \begin{pmatrix} -n_p \omega_r i_q - \frac{Mr_r i_q^2}{Lr_\psi} + U_{flux} \\ n_p \omega_r i_d + \frac{n_p \omega_r M_\psi}{\sigma_{Lr}} + U_{speed} \end{pmatrix}$$

$$\begin{pmatrix} v_{qs} \\ v_{ds} \end{pmatrix} = \psi \begin{pmatrix} \lambda_{dr} & \lambda_{qr} \\ -\lambda_{qr} & \lambda_{dr} \end{pmatrix}^{-1} \begin{pmatrix} v_d \\ v_q \end{pmatrix} \quad (5)$$

And

$$\sigma = \frac{L_s L_r - M^2}{L_R}$$

The unwanted nonlinear terms cancel, and the closed loop dynamic system equations become similar to that of a dc motor, as seen in (6). The quadrature axis current represents the speed-producing element, while the direct axis current represents the torque-producing element. As revealed in (6), and i_d, i_q are asymptotically decoupled in this reference frame. This will allow the user to independently control their steady-state values as well as their dynamic performance. The only downside of FOC is the nonlinear nature of ρ and the fact that it is already very difficult to estimate accurately. This is a common downside of many field-oriented controllers.

$$\frac{d_{\omega r}}{dt} = \frac{3n_p M\psi i_q}{2Jl_2} - \frac{T_{load}}{J}$$
$$\frac{d\psi}{dt} = -\frac{r_r\psi}{L_r} - \frac{r_r M i_d}{L_r}$$
$$\frac{di_q}{dt} = -\left(\frac{M^2 r_r}{\sigma L_r^2} + \frac{r_s}{\sigma}\right) i_q + U_{speed}$$
$$\frac{di_d}{dt} = -\left(\frac{M^2 r_r}{\sigma L_r^2} + \frac{r_s}{\sigma}\right) i_d + \frac{r_r M\psi}{L_r} + U_{flux}$$
$$\frac{dp}{dt} = n_p\omega_r + \frac{r_i M i_d}{L_r\psi} \quad (6)$$

3. Indirect field-oriented control stability analysis

Since IFOC relies on the use of an estimated stator flux, the observer must be proved to be stable in the sense of Lyapunov. It would be prudent to see if a solution exists that makes the control scheme globally asymptotically stable (GAS) using Lyapunov's second method. With this method, it is required—just as in the DTC case—that the Lyapunov function (LF) is positive definite and its derivative is negative definite. In this case, the candidate LF given in (7) is composed from four positive semi-definite matrices in (8) [26]. This candidate LF is only valid if R_r is identically $\widehat{R_r}$. All of the a and b values below are positive constants, made up of combinations of resistance and gain values.

$$V(w) = \frac{1}{2} w^T p w \quad (7)$$

$$P = (z_1 + z_2)P_1 + \left(\frac{K_1 + R_r^2 K_1}{R_r}\right) P_2 + P_3 + P_4$$

$$where\ P_1 = \begin{bmatrix} 1 & 0 & 0 & 0 \\ 0 & 1 & 0 & 0 \\ 0 & 0 & 0 & 0 \\ 0 & 0 & 0 & 0 \end{bmatrix}, P_2 = \begin{bmatrix} \frac{1}{\hat{R}_r} & 0 & 0 & -1 \\ 0 & 0 & 0 & 0 \\ 0 & 0 & 0 & 0 \\ -1 & 0 & 0 & \hat{R}_r \end{bmatrix}, P_3 = \begin{bmatrix} 0 & 0 & 0 & 0 \\ 0 & 0 & 0 & 0 \\ 0 & 0 & 1 & k_p \\ 0 & 0 & k_p & k_p^2 \end{bmatrix}, P_4 = \begin{bmatrix} k_p^2 & 0 & kp^h & 0 \\ 0 & 0 & 0 & 0 \\ kp^h & 0 & h^2 & 0 \\ 0 & 0 & 0 & 0 \end{bmatrix} \quad (8)$$

K_p is the proportional constant
H is a positive constant

$$z_1 = \frac{b_{13}^2}{R_{ra3}}\ and\ z_2 = \frac{b_{14}^2}{R_{ra4}}$$

The derivative of this candidate LF is shown in (9). Assuming that all a and b constants are positive, the derivative of the candidate LF is shown in [9] to be always negative, or negative definite. This along with the fact that the candidate LF is positive definite makes it an LF.

$$\dot{V}(w) = -a_1 w_1^2 - a_3 w_3^2 - a_4 w_4^2 - 2b_{13 w_1 w_3} + 2b_{14 w_1 w_4} - \left(\frac{b_{13}^2}{a_3} - \frac{b_{14}^2}{a_4}\right) w_1^2 - \left(\frac{b_{13}^2}{a_3} - \frac{b_{14}^2}{a_4}\right) w_2^2 \quad (9)$$

For the other case where R_r is not identically equal to $\widehat{R_r}$, the proposed candidate LF from [5] is shown in (10). The same constituent P matrices in the previous case are again used in this candidate LF. The derivative of this candidate LF is shown in (11), where the constants ε_1 and ε_2 are off-diagonal coefficients for the constant symmetric matrix $Q(\varepsilon_1, \varepsilon_2)$. Since $Q(\varepsilon_1, \varepsilon_2)$ is shown to be positive definite, the derivative is negative definite, and the candidate LF is indeed an LF as long as the estimated rotor resistance is correct within 100%. By insuring this condition, all of the signals in the system will remain bounded.

$$V(w) = w^T \left(\frac{1}{2}p_1 + .1p_2 + p_3 + p_4\right) w \tag{10}$$

$$\dot{V(w)} = -w^T Q(\varepsilon_1, \varepsilon_2) w$$

$$where\ \varepsilon_1 = \frac{R_r\beta^2 - \hat{R}_r\overrightarrow{V_2}}{2R_r\beta^2}\ and\ \varepsilon_2 = \frac{\hat{R}_r\overrightarrow{V_1}}{2R_r\beta^2} \tag{11}$$

Indirect field-oriented control parameter sensitivity

When IFOC is used with current control or with SVPWM, it is dependent on the rotor leakage inductance, L_{lr}, magnetizing inductance, L_m , and the rotor resistance, r_r. Again, it is possible to build a Jacobian matrix, J_{IFOC}, in which the sensitivities of torque, speed, and other desired variables or outputs are estimated relative to change in motor parameters. For IFOC, the Jacobian matrix is expected to be (12).

$$\begin{pmatrix} \Delta T^e \\ \Delta\omega_{rm} \end{pmatrix} = J_{IFOC} \begin{pmatrix} \Delta L_{lr} \\ \Delta L_m \\ \Delta r_r \end{pmatrix}$$

$$where\ J_{IFOC} = \begin{pmatrix} \frac{\partial T^e}{\partial r_{lr}} & \frac{\partial T^e}{\partial L_m} & \frac{\partial T^e}{\partial r_r} \\ \frac{\partial \omega_{rm}}{\partial r_{lr}} & \frac{\partial \omega_{rm}}{\partial L_m} & \frac{\partial \omega_{rm}}{\partial r_r} \end{pmatrix} \tag{12}$$

It is important here to consider torque and speed ripple under switching control for both IFOC and DTC. While the sensitivity analyses would result in steady-state variations ΔT^e and Δw_{rm}, dynamic variations can also result from switching. For example, for a given stator current under hysteretic switching, the formulations of the above Jacobian matrices are not trivial. If the stator current is i_s given by $i_s = I_s + \Delta i_s$, where Δi_s is the width of the hysteresis band and I_s is the desired stator current, then the expected T^e and ω_{rm} are given by (13) and (14), respectively. They are both broken into two terms: the offset, or average component, and the hysteresis band component.

$$T^e = T^e_{(offset)} + \Delta T^e_{(hys)} \tag{13}$$

$$\omega_{rm} = \omega_{rm(offset)} + \Delta\omega_{rm(hys)} \tag{14}$$

Denoting the time average of a variable x as $\langle x \rangle$ the resulting averages would be those in (15) and (16).

$$\langle T^e \rangle = \langle T^e_{(offset)} \rangle + \langle \Delta T^e_{(gys)} \rangle \tag{15}$$

$$\langle \omega_{rm} \rangle = \langle \omega_{rm(offset)} \rangle + \langle \Delta\omega_{rm(hys)} \rangle \tag{16}$$

An offset will not occur if $\langle \Delta T^e{}_{(hys)} \rangle$ and $\langle \Delta\omega_{rm(hys)} \rangle$ are zero, but zero-average ripple is not guaranteed in general and must rely on integral gain in the loop controls. The block diagram for an IFOC motor drive with current hysteresis as the switching scheme is shown in Figure 1. This combination is by far the most common higher-performance drive used in industry. The commanded

signals are the torque,T^{e*}, and direct axis rotor flux, λ_{dr}^{e*}, which differs from the DTC motor controller that uses the absolute value of the total stator flux. The torque and rotor flux commands are converted into the quadrature and direct stator current variables and then compared to the measured induction motor currents that are fed back. The induction motor in the block diagram is represented by the circle with the label "IM".

The second switching scheme that is analyzed with IFOC is SVPWM. The block diagram for this topology can be found in Figure 2. The difference between this topology and the previous current hysteretic IFOC topology is that the quadrature and direct voltages are used in the switching scheme instead of the currents. To get these voltages, the equations labeled "1" and "2" in Figure 2 are shown in (17) and (18) [9].

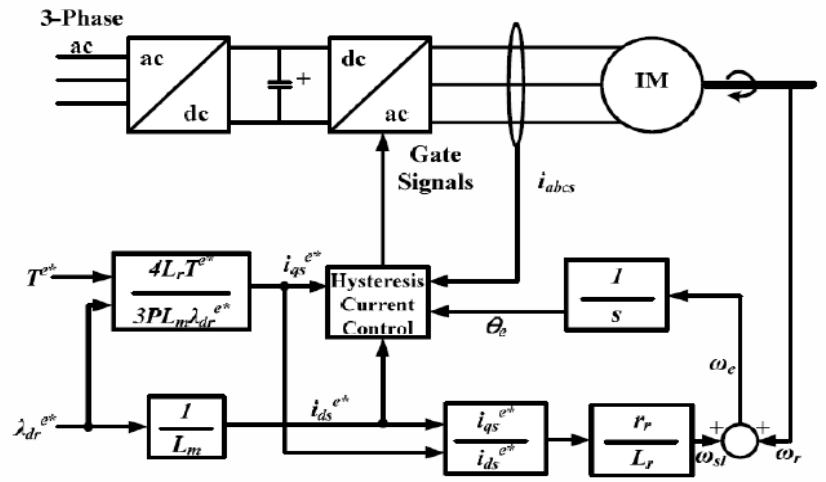

Figure 1: Block Diagram of IFOC with Current Hysteresis [9]

$$v_{qs}^{s} *= \sigma\left\{-\frac{p}{2}\omega_r i_{ds}^{s} - \frac{L_m}{\tau_r} i_{ds}^{s} \frac{(i_{qs}^{s}\lambda_{ds}^{s} - i_{ds}^{s}\lambda_{qr}^{s})}{(\lambda_s^s)^2} - \frac{\lambda_{dr}^{s}\omega_{rm}^{*}}{\lambda_s^s} + \frac{\lambda_{qr}^{s}\lambda_s^{*}}{\lambda_r^s}\right\} - \frac{L_m p \omega_r \lambda_{dr}^{s}}{2L_r} \quad (17)$$

$$v_{ds}^{s} *= \sigma\left\{-\frac{p}{2}\omega_r i_{qs}^{s} - \frac{L_m}{\tau_r} i_{qs}^{s} \frac{(i_{qs}^{s}\lambda_{dr}^{s} - i_{ds}^{s}\lambda_{qr}^{s})}{(\lambda_r^s)^2} - \frac{\lambda_{dr}^{s}\omega_{rm}^{*}}{\lambda_r^s} + \frac{\lambda_{dr}^{s}\lambda_s^{*}}{\lambda_r^s}\right\} - \frac{L_m p \omega_r \lambda_{qr}^{s}}{2L_r} \quad (18)$$

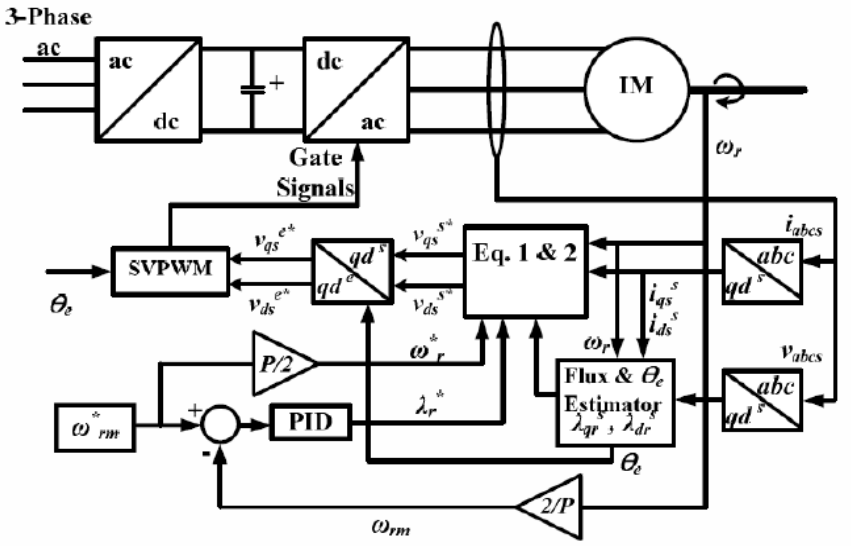

Figure 2: Block Diagram of IFOC-SVPWM [9]

4. Results and Discussion

Now that the standard topologies have been discussed, the parameter sensitivity results will be revealed. Standard IFOC is sensitive to the rotor leakage inductance, L_{lr} , magnetizing inductance, L_m, and rotor resistance, r_r, as discussed in the previous section. By visual inspection of Figure 3, one can see that by increasing or decreasing the rotor leakage inductance by 25% from the nominal value, there is minimal change in the torque response. Figure 4 shows a totally different story: when the magnetizing inductance is decreased by 25% from its nominal value, the steady state average torque output increases to 6.93 N-m, or a 38.6% increase over the desired torque command of 5 N-m. When the magnetizing inductance is increased by 25%, the steady state decreases to 4.37 N-m, which is a 12.6% decrease from the desired torque. The last parameter that has any sensitivity to change is the rotor resistance. Figure 5 shows the change in performance of standard IFOC when the rotor resistance is increased and decreased 25% from the nominal value. Increasing the rotor resistance by 25% will affect the rotor time constant and therefore increase the torque response so that there is an overshoot, while a decrease of 25% leads to a torque response that is overdamped and therefore an undershoot occurs. There are also steady-state torque errors for both cases, which is a very undesirable effect. In conclusion, the only two parameters that seem to have a high sensitivity for standard IFOC are the magnetizing inductance and the rotor resistance.

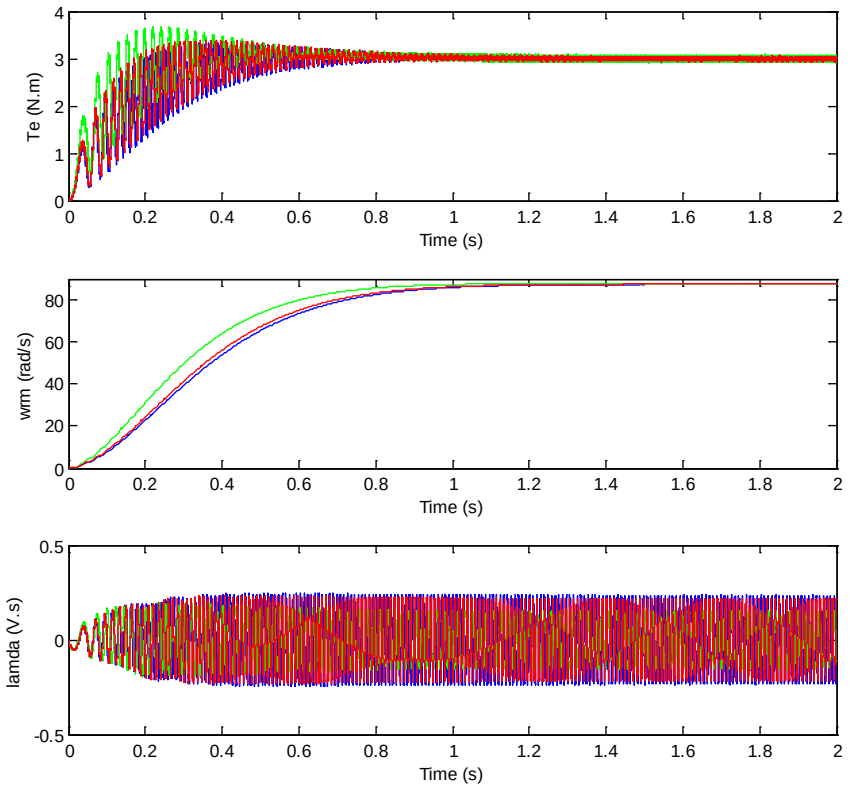

Figure 3: IFOC, Sensitivity to L_{lr}

Now that standard IFOC has been examined, it is useful to look at the parameter sensitivity of IFOC but with a different switching scheme: SVPWM. As shown In the previous section, IFOC-SVPWM is sensitive to the change in rotor leakage inductance, L_{lr}, rotor self inductance, L_r , magnetizing inductance, L_m , and rotor resistance, r_r. The sensitivity from a change in the rotor leakage inductance is shown in Figure 6. The sensitivity from a 25% decrease or increase in the rotor leakage inductance is very low, since the altered parameter performance is almost identical to the nominal performance. As

for the sensitivity for the magnetizing inductance, when the error is 25% greater than the nominal value, the torque gets to steady-state quicker, but there is a steady-state error where it is 0.23 N-m lower than commanded (Figure 7). The case where the error is 25% lower than the nominal value is almost identical to the nominal case, as can be seen in Figure 7.

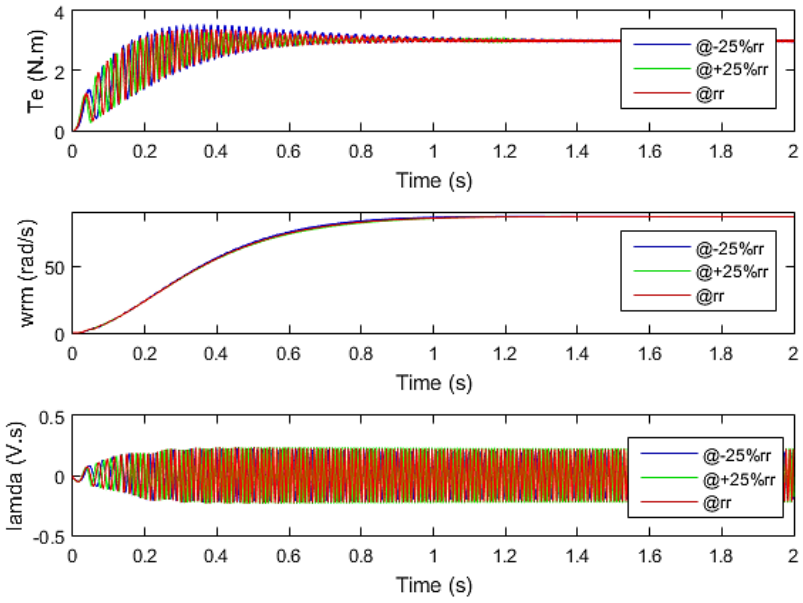

Figure 4: IFOC, Sensitivity to L_m

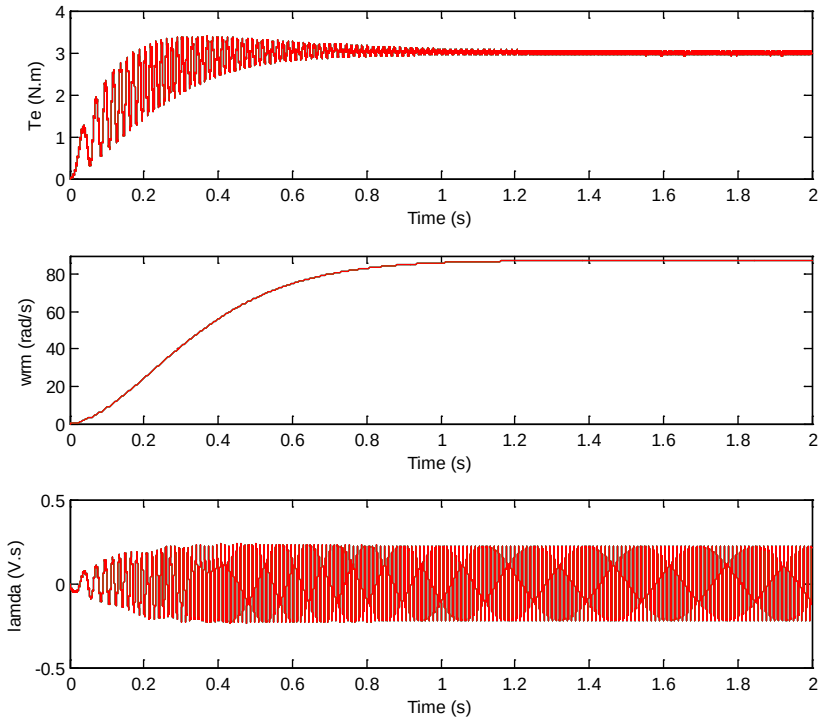

Figure 5: IFOC, Sensitivity to r_r

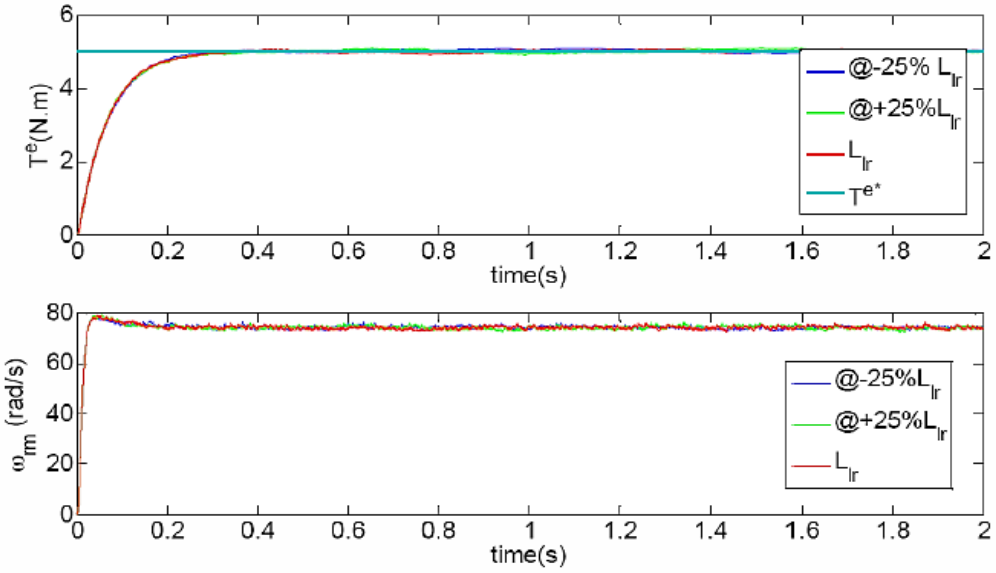

Figure 6: IFOC-SVPWM, Sensitivity to L_{lr}

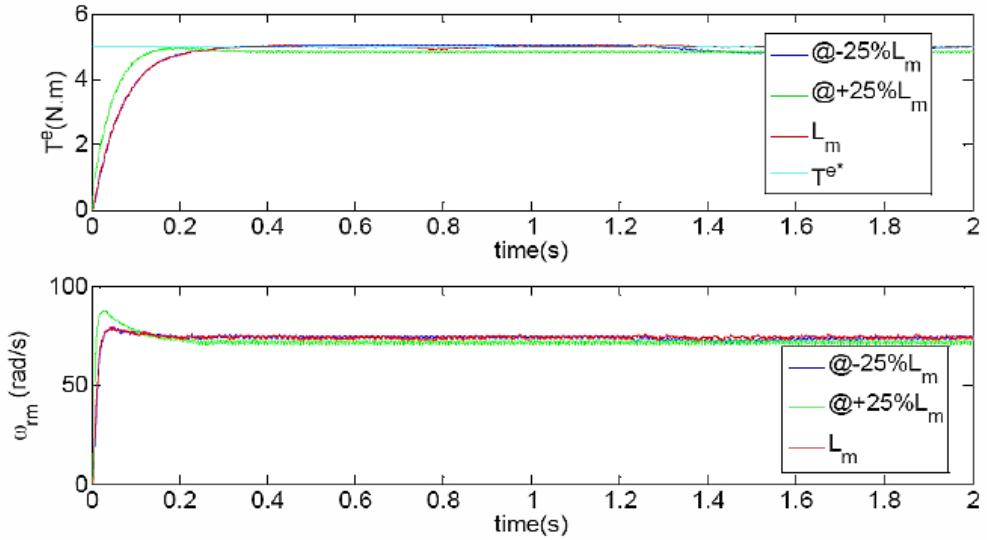

Figure 7: IFOC-SVPWM, Sensitivity to L_m

Another parameter that was analyzed in previous section for a sensitivity analysis was the rotor inductance. Figure 8 shows that the torque performance is very insensitive to any changes in the rotor inductance—the altered cases are virtually identical to the unaltered case. The last parameter that was tested in the IFOC-SVPWM parameter sensitivity analysis is the rotor resistance. Figure 9 shows the sensitivity results for this parameter. There seems to be a very low sensitivity to any change in the rotor resistance, which was slightly unexpected. Therefore, the only parameter for IFOC-SVPWM that seems to affect performance is the magnetizing inductance.

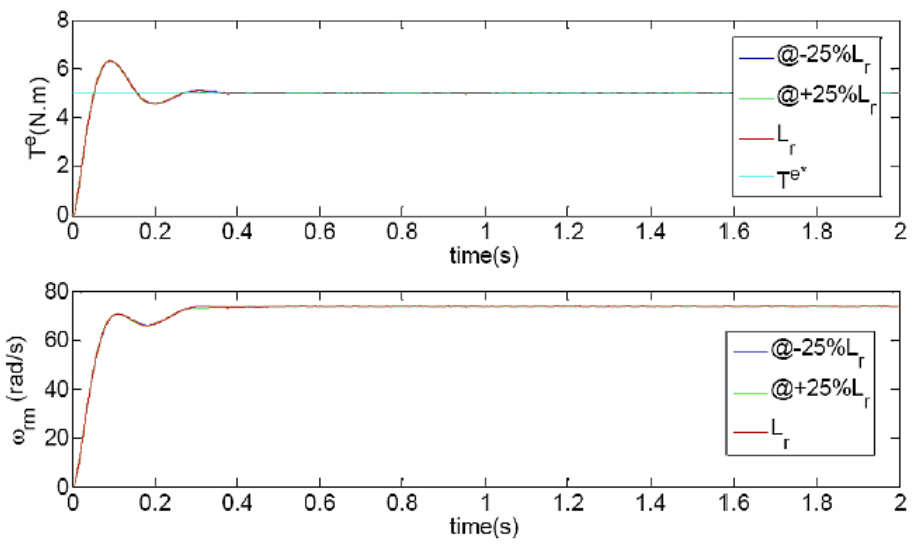

Figure 8: IFOC-SVPWM, Sensitivity to L_r

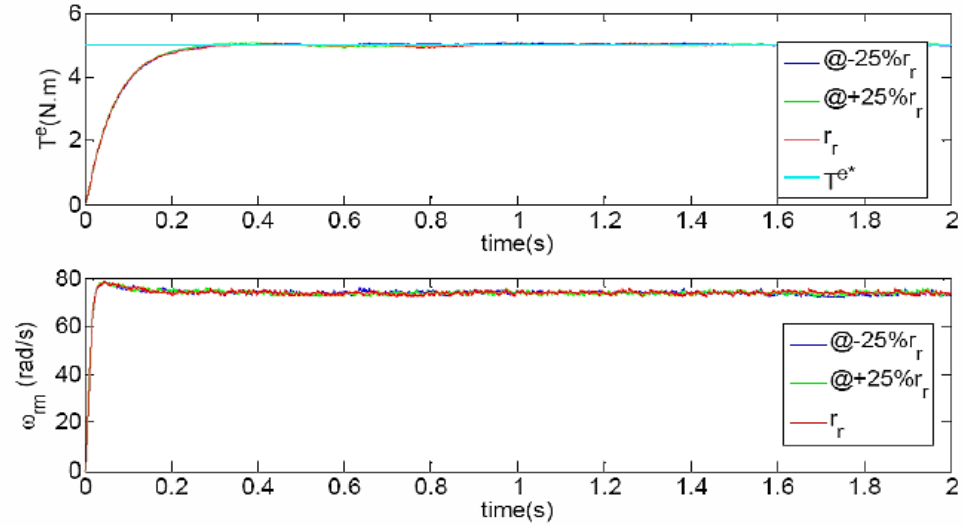

Figure 9: IFOC-SVPWM, Sensitivity to r_r

The dynamic performances of DTC and IFOC are both affected significantly by the choice of switching scheme. These PID gains were tuned for best performance for each of the drives. IFOC-SVPWM performs much better than IFOC with hysteretic control; for instance, the torque overshoot is much less with SVPWM—less than 0.5%, compared to 14%—since the system is almost critically damped with the chosen gains under SVPWM. DTC-SVPM has a deterioration of performance—26% torque overshoot compared to 0% with the standard six sector switching table. The worst case IFOCSVPWM speed overshoot is 40.6%, while DTC-SVPWM has only a 9.4% speed overshoot. The torque settling time of IFOC-SVPWM in this case has noticeably reduced to about 0.3 s, and the DTC-SVPWM torque settling time has become a good deal longer—about 0.3 s compared to 15 ms in the case with the switching table. The speed settling times are also about 0.3 s for both DTC and SVPWM. Based on this more direct comparison using the same switching scheme, there is no clear distinction as to which method to choose for a better torque step performance. It is shown that when the drive and switching scheme are totally decoupled, the performances can be very dissimilar; IFOC-SVPWM performs much better than the classic IFOC using current hysteresis. From these results, it looks as if IFOC performs slightly better than DTC using the same switching technique, in this case SVPWM. This does not mean it is a better drive overall, since there may be a different switching scheme that yields

a different result. For instance, IFOC may turn out to be inferior to DTC when using a switching table as the preferred switching scheme. Therefore, the results are still inconclusive as to which of the four drives has the best torque response because of the many switching schemes that can be applied to each drive. The numerous permutations between motor drives and switching schemes do not allow for a timely and thorough analysis.

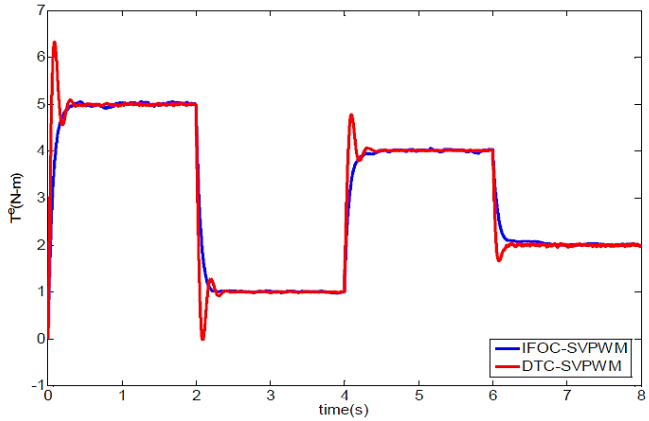

Figurer 10: Torque Response of DTC-SVPWM and IFOC-SVPWM to a Driving

Cycle

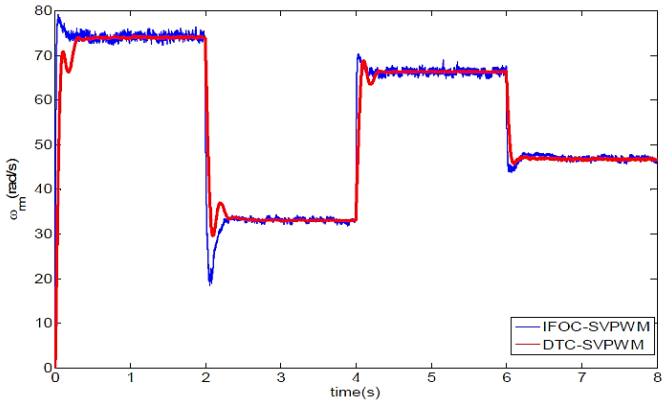

Figure 11: Speed Response of DTC-SVPWM and IFOC-SVPWM to a Driving

Cycle

5. CONCLUSIONS AND FUTURE WORK

In this study, the work analyzes and compares different motor controllers using a second order motor loade. Basic Principles of vector control and mathematical modeling of induction motor are discussed. An algorithm along with block diagram for the vector control is lucidly presented. The obtained results are found in line with the expectations The tests that were chosen are: speed step, torque step and position command of the motor drive. From these results, it looks IFOC has a comparable torque response when SVPWM is used for the switching scheme in place of the standard current hysteretic switching. There seems to be a very low sensitivity to any change in the rotor resistance, which was slightly unexpected. In order to overcome this problem, should a study to apply new methods to estimate the online resistance operations , this method in a state of permanent, transient , the functions of the low - speed , and zero , and improve. Also, using an enhanced flux observer might improve convergence times. In the future “inner loop” control, or control using currents, voltages and fluxes, versus “outer loop” control, or one that uses torques and speeds, should be analyzed to help in the design of improved motor controllers.

References

[1] A. M. Bazzi, A. P. Friedl, S. Choi, and P. T. Krein, "Comparison of induction motor drives for electric vehicle applications: dynamic performance and parameter sensitivity analyses," in IEEE International Electric Machines and Drives Conference Proceedings, 2009, pp. 639-646.

[2] C. A. Martins and A. S. Carvalho,"Technological trends in induction motor electrical drives," in IEEE Power Technology Conference Proceedings, 2001,vol. 2, pp. 7-12.

[3] M. Cruz, A. Gallegos, R. Alvarez, and F. Pazos, "Comparison of several nonlinear controllers for induction motors," in IEEE International Power Electronics Conference, 2004, pp. 134-139.

[4] M. P. Kazmierkowski and A. B. Kasprowicz, "Improved direct torque and flux vector control of PWM inverter-fed induction motor drives," IEEE Transactions on Industrial Electronics, vol. 42, no 4, pp. 344-350, Aug. 1995.106

[5] M. Vasudevan and R. Arumugam, "Different viable torque control schemes of induction motor for electric propulsion systems," in IEEE Industry Applications Conference, 2004, pp. 2728-2737.

[6] P. C. Krause, Analysis of Electric Machinery. New York, NY: McGraw-Hill, 1986.

[7] R.Marino, I. Kanellakopoulos, and P. Kokotovic, "Adaptive tracking for feedbacklinearizable SISO systems," in Proceedings of the 28th IEEE Conference on Decision and Control, Tampa, FL, Dec. 1989, pp. 1002-1007.

[8] S. Sastry and A. Isidori,"Adaptive control of linearizable systems," IEEE Trans. on Automatic Control, vol. 34, no. 11, pp. 1123-1131, Nov. 1989.

[9] T. A. Wolbank, A. Moucka, and J. L. Machl, "A comparative study of fieldoriented and direct-torque control of induction motors reference to shaftsensorless control at low and zero- speed," in Proceedings of the 2002 IEEE International Symposium on Intelligent Control, 2002, pp. 391-396.

Authors

Peyman jabraelzade received MSc degrees in Mechatronics Engineering from Islamic Azad university, Ahar, IRAN, in 2014. Areas of his research interests include optimization techniques, intelligent systems, Image Processing, manufacturing and mechatronics.

Neda pourghanbar recived the MSc degrees in Electrical Engineering from Islamic Azad university, Ahar, IRAN, in 2016. Areas of his research interests include optimization techniques, intelligent systems, Image Processing, manufacturing and mechatronics.